

Effect of spin-orbit interaction on the plasma excitations in a quantum wire

Godfrey Gumbs

*Department of Physics and Astronomy, Hunter College of the City University of New York, 695 Park Avenue,
New York, New York 10021, USA*

(Received 29 June 2004; published 10 December 2004)

Incorporating the spin-orbit interaction into the Hamiltonian of a quantum wire, we have calculated the plasma excitation energies. We include both the Rashba term (α coupling) arising from the asymmetry of the heterostructure forming the two-dimensional electron gas, and the β coupling due to the quantum wire confinement which we model with a harmonic potential. The α coupling lifts the degeneracy of the spin states and the β coupling causes the quantized transverse single-particle energy to have negative dispersion. Our model yields several interesting features which may be observed with the use of inelastic light scattering and electron energy loss spectroscopy (EELS). The collective excitations for the quantum wire are determined by the allowed transitions between subbands. The collective plasma excitations split off from each branch of allowed particle-hole modes. The subband structure gives rise to a plasmon mode with a negative group velocity.

DOI: 10.1103/PhysRevB.70.235314

PACS number(s): 71.70.Ej, 73.20.Mf, 68.65.La

I. INTRODUCTION

Recently, one-dimensional (1D) electronic systems (ES's), i.e., quantum wires, have been fabricated from originally two-dimensional (2D) ES's, e.g., GaAs/Al_xGa_{1-x}As heterostructures, by techniques involving deep mesa etching.¹⁻³ Whenever the length scales of lateral confinement and the de Broglie wavelength are comparable, there is lateral quantization (LQ) which in turn gives rise to a set of discrete 1D subbands for the free electron motion along the wires.⁴⁻⁸ When a perpendicular ambient magnetic field B is applied, Landau quantization and lateral quantization are coupled to one another to form discrete 1D Landau-subbands (LS's).

In the present paper, we study the effect of spin-orbit (SO) coupling in a quantum wire in the absence of an external magnetic field. We include the contributions to the SO interaction from the Rashba effect⁹⁻¹² due to the asymmetry of the quantum well from which the quantum wire is fabricated as well as a contribution from the lateral confinement, first pointed out by Moroz and Barnes.¹³ Both the single-particle properties, such as the electron energy levels, Fermi energy, level occupation number, as well as the collective excitations of a quantum wire are of interest. Our present formalism is suitable for interpreting and predicting experimental data. The first step is to calculate the single particle wave functions and energy eigenvalues for a quantum wire system with parabolic confinement.¹³ For weak Rashba coupling, we may use perturbation theory to obtain approximate results for the eigenstates for such a model. Our results can be employed in a generalized formalism for the collective excitations of a multiwire array with tunneling^{14,15} under strong or weak modulation.

The motivation for the present study is due to the recent work of Moroz and Barnes¹³ who reported interesting features in the conductance due to SO interactions in a quantum wire. The model for the wire corresponds to strong lateral confinement by applying a depletion gate voltage V_g in one direction between the 2D ES and grating gate. In an experi-

ment, both the modulation strength and areal electron density \bar{n}_s can be changed by varying V_g . For small negative values of V_g , the experiments should show a decrease in the excitation energy due to a decrease of \bar{n}_s in the 2D regime.

The main results of this paper are as follows. In our calculated results, we chose a Fermi energy E_F for which only the lowest subband is occupied at $T=0$ K. In the model, harmonic confinement is assumed in the transverse direction for the infinitely long wire. We show explicitly how the SO coupling affects both the plasmon modes and single-particle excitations (SPE's), arising from transitions from the ground subband. The SPE's consist of branches corresponding to the spin being flipped or remain unchanged during an intrasubband or intersubband transition from below to above E_F . The Coulomb interaction causes a plasmon excitation to split off from the particle-hole SPE modes. In addition, we show that Landau damping plays a key role in the allowed transitions contributing to the plasma modes. When there is no SO interaction present in the quantum wire, the lowest plasmon arises from transitions from the ground subband to excited states whose band edges are determined by the transverse quantum confinement. In the presence of SO coupling, this mode is dramatically modified in two ways. First, it anticrosses with a lower intrasubband plasmon mode. Secondly, it has a negative group velocity for a range of values of the longitudinal wave vector. We explain the anticrossing and negative group velocity as being due to the lifting of the degeneracy of the transverse energy subbands ϵ_x by the Rashba SO interaction and the dispersion of ϵ_x produced by the SO coupling arising from the parabolic confining potential.

The rest of this paper is organized as follows. In Sec. II, we present our model Hamiltonian for the quantum wire with SO coupling and briefly derive the dispersion equation for plasma oscillations. Section III is devoted to numerical results for the plasma excitations. We conclude with some comments in Sec. IV.

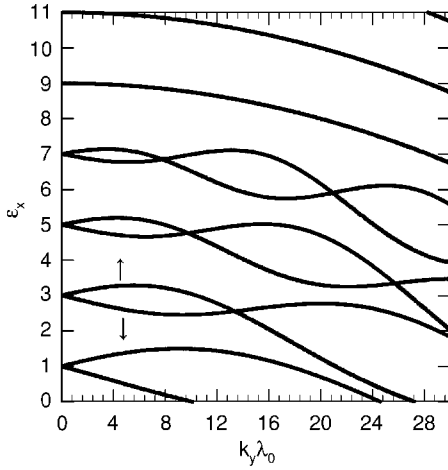


FIG. 1. The transverse energy eigenvalues $\epsilon_x = 2\epsilon_{k_y, n}/\hbar\Omega - k_y^2\lambda_0^2$ as a function of $k_y\lambda_0$ for $\lambda_0/l_\alpha = 0.1$ and $\lambda_0/l_\beta = 0.1$. The degeneracy of the \uparrow - and \downarrow -spin levels is lifted for finite k_y by the Rashba SO term in the Hamiltonian in Eq. (1).

II. MATHEMATICAL FORMULATION OF THE PROBLEM

In this section, we derive the dispersion relation for plasma oscillations when spin-orbit interactions are present in a quantum wire located in the x - y plane. We also restrict ourselves to a model in which electrons with effective mass m^* are confined by a parabolic potential $\frac{1}{2}m^*\Omega^2x^2$ in the x direction. The effective mass Hamiltonian for an infinitely long wire in the y direction is

$$\mathcal{H} = \frac{\hat{\mathbf{p}}^2}{2m^*} + \frac{m^*}{2}\Omega^2x^2 + \frac{\alpha}{\hbar}(\hat{\sigma} \times \hat{\mathbf{p}})_z + \frac{\beta}{\hbar\lambda_0}(\hat{\sigma} \times \hat{\mathbf{p}})_x, \quad (1)$$

where $\hat{\mathbf{p}}$ is the momentum operator and $\hat{\sigma} = \{\sigma_x, \sigma_y, \sigma_z\}$ is the vector of Pauli spin matrices. The spin-orbit interaction in Eq. (1) has two contributions. One of them arises from the asymmetry of the quantum well, i.e., the Rashba mechanism⁹⁻¹² and is described by the term involving the parameter α . The value of α depends on the material¹⁶⁻¹⁹ and lies within the range $(1-12) \times 10^{-10}$ eV cm. The second contribution to the SO interaction arises as a result of the parabolic confining potential. This is given by the last term in Eq. (1) with $\lambda_0 = (\hbar/m^*\Omega)^{1/2}$ a characteristic length and β a SO-coupling parameter introduced by Moroz and Barnes,¹³ who estimated β to be about ten percent that of α .

Determining the eigenfunctions $\Psi = \Psi(\mathbf{r})$ and eigenvalues ϵ of the Schrödinger equation $\mathcal{H}\Psi(\mathbf{r}) = \epsilon\Psi(\mathbf{r})$ is the natural first step in our calculations. These calculations have been discussed in detail in Ref. 13. The wave function $\Psi = \{\Psi_\uparrow(\mathbf{r})\Psi_\downarrow(\mathbf{r})\}$ is a two-component spinor where the eigen-solutions may be expressed as $\Psi_\sigma(\mathbf{r}) = (e^{ik_y y}/\sqrt{L_y})\Phi_\sigma(X)$ since the Hamiltonian (1) is translationally invariant in the y direction. In this notation, L_y is a normalization length, $X = x/\lambda_0$ is a dimensionless coordinate, and k_y is a wave vector parallel to the wire direction.

In Fig. 1, we have plotted the dimensionless transverse energy eigenvalues, i.e., $\epsilon_x = 2\epsilon/(\hbar\Omega) - k_y^2\lambda_0^2$, as a function of $k_y\lambda_0$, for $\lambda_0/l_\alpha = 0.1$ and $\lambda_0/l_\beta = 0.1$. In this notation, l_α

$= \hbar^2/(2m^*\alpha)$ and $l_\beta = \hbar^2/(2m^*\beta)$. As Fig. 1 shows, the lowest energy levels corresponding to $n=0, 1, 2$, and 3 clearly have their degeneracy lifted on the scale shown in the plot. This splitting is due to the α coupling from the Rashba SO interaction. The splitting of the \uparrow - and \downarrow -spin energy eigenvalues is decreased as the quantum number $n \geq 4$, in this case, increases as shown in Fig. 1. For weak α coupling $\lambda_0/l_\alpha \ll 1$, the energy eigenvalues are approximately given by $2\epsilon_{k_y, n, \sigma}/\hbar\Omega \approx k_y^2\lambda_0^2 + 2n + 1 - \frac{1}{4}X_\beta^2 + \sigma\delta\epsilon_{k_y, n}$, where $\sigma = \pm 1$, $X_\beta = \lambda_0^2 k_y/l_\beta$. Also, the term $\delta\epsilon_{k_y, n}$ is due solely to the α coupling and the effect of β coupling is to make the transverse energy $\epsilon_x \equiv 2\epsilon_{k_y, n}/\hbar\Omega - k_y^2\lambda_0^2$ dependent on the wave vector k_y . Clearly, in the absence of α coupling, the group velocity in the y direction is negative. Also, to lowest order in perturbation theory, we have $\delta\epsilon_{k_y, n} = \sqrt{\langle \phi_\downarrow^{(n)} | \hat{P}_- | \phi_\uparrow^{(n)} \rangle \langle \phi_\uparrow^{(n)} | \hat{P}_+ | \phi_\downarrow^{(n)} \rangle}$, with $\hat{P}_\sigma(k_y) = (\lambda_0/l_\alpha)(\sigma d/dX + k_y\lambda_0)$. We have introduced harmonic oscillator wave functions

$$\begin{aligned} \phi_{\uparrow\downarrow}^{(n)}(X) &\equiv \Phi_{\uparrow\downarrow}^{(n)}(X)|_{\lambda_0/l_\alpha=0} \\ &= \frac{1}{\sqrt{\pi^{1/2}2^n n!}} e^{-(1/2)[X \mp (1/2)X_\beta]^2} H_n\left(X \mp \frac{1}{2}X_\beta\right). \end{aligned} \quad (2)$$

With the use of standard many-body theory,¹⁴ the dispersion relation for plasmons can be obtained in the random-phase approximation (RPA). If the quantum wire is embedded in a medium with effective background dielectric constant ϵ_b , then the in-plane Fourier transform of the induced electrostatic potential $\tilde{\varphi}$ satisfies Poisson's equation which may be written as

$$\left(\frac{\partial^2}{\partial z^2} - q_\parallel^2\right)\tilde{\varphi}(q_\parallel, z; \omega) = \delta(z)P(q_\parallel, \omega), \quad (3)$$

where q_\parallel is the in-plane wave vector and

$$\begin{aligned} P(q_\parallel, \omega) &= \frac{4\pi e}{\epsilon_s L_y} \sum_{k_y} \sum_{n, n'} \sum_{\sigma, \sigma'} \langle k_y, n, \sigma | \hat{\rho}_1 | k_y - q_\parallel, n', \sigma' \rangle \\ &\quad \times F(q_x; k_y - q_\parallel, n'; k_y, n), \end{aligned} \quad (4)$$

with $\epsilon_s = 4\pi\epsilon_0\epsilon_b$ and the form factor integral is defined by

$$\begin{aligned} F(q_x; k'_y, n'; k_y, n) &= \int_{-\infty}^{\infty} dX e^{-iq_x X} [\Phi_\uparrow^*(X, k'_y, n')\Phi_\uparrow(X, k_y, n) \\ &\quad + \Phi_\downarrow^*(X, k'_y, n')\Phi_\downarrow(X, k_y, n)]. \end{aligned} \quad (5)$$

The matrix element of the perturbed density matrix $\hat{\rho}_1$ is

$$\begin{aligned} \langle k_y, n, \sigma | \hat{\rho}_1 | k'_y, n', \sigma' \rangle &= e^{\frac{f_0(\epsilon_{k_y, n, \sigma}) - f_0(\epsilon_{k'_y, n', \sigma'})}{\hbar\omega + \epsilon_{k'_y, n', \sigma'} - \epsilon_{k_y, n, \sigma}}} \\ &\quad \times \langle k_y, n | \tilde{\varphi} | k'_y, n', \sigma' \rangle, \end{aligned} \quad (6)$$

where $f_0(\epsilon)$ is the Fermi-Dirac distribution function. The continuity of the induced potential and the discontinuity of

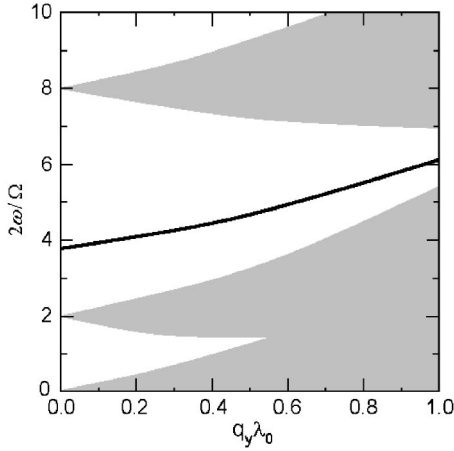


FIG. 2. For $\alpha=0$ and $\beta=0$, the normalized frequencies $\bar{\omega} = 2\omega/\Omega$ of the plasmon excitations and particle-hole modes are plotted as a function of $q_y\lambda_0$. The values for m^* , ϵ_b , and E_F are given in the text. The shaded regions denote the single-particle excitations giving rise to Landau damping.

its derivative at $z=0$ together yield $\tilde{\varphi}(q_{\parallel}, z; \omega)$ as the solution of Eq. (3) with $\tilde{\varphi}(q_{\parallel}, z=0; \omega) = -P(q_{\parallel}, \omega)/2q_{\parallel}$. Making use of this result in Eqs. (4) and (6), we obtain the following equation for determining the induced electrostatic potential within the $z=0$ plane:

$$\tilde{\varphi}(q_x, q_y; \omega) + \frac{2\pi e^2}{\epsilon_s q_{\parallel}} \frac{1}{L_y} \sum_{k_y} \sum_{n, n'} \Pi_{n, n'}(q_y, k_y; \omega) F(q_x; k_y - q_y, n'; k_y, n) \tilde{\varphi}(k_x, q_y; \omega), \quad (7)$$

where the polarization function is given by

$$\Pi_{n, n'}(q_y, k_y; \omega) = \sum_{\sigma, \sigma'} \frac{f_0(\epsilon_{k_y, n, \sigma}) - f_0(\epsilon_{k_y - q_y, n', \sigma'})}{\hbar\omega + \epsilon_{k_y - q_y, n', \sigma'} - \epsilon_{k_y, n, \sigma}}. \quad (8)$$

The plasma modes correspond to the nontrivial solutions of Eq. (7). We now present numerical results for the plasmons and the single-particle excitations.

III. NUMERICAL RESULTS FOR THE PLASMON EXCITATIONS AND PARTICLE-HOLE MODES

Since our aim is to understand the effect of spin-orbit interaction on the charge density excitations in a quantum wire, we plot in Fig. 2 the dispersion relation at $T=0$ K in the absence of either spin-orbit α or β coupling. Scaling all energies in units of $\hbar\Omega/2$, we chose the Fermi energy $E_F = 2(\hbar\Omega/2)$ which corresponds to only the lowest degenerate subband being occupied. On this energy scale, the transverse energy levels occur at $2n+1$, where $n=0, 1, 2, 3, \dots$. In the long wavelength limit $q_y\lambda \rightarrow 0$, the excitation energies correspond to transitions between the transverse energy levels $\bar{\omega} \equiv 2\omega/\Omega \approx 2|n-n'|$, where n and n' are zero or a positive integer. For our choice of E_F , the boundaries of the particle-hole mode regions are given by $2|n-n'| + (q_y\lambda_0 \pm 2)q_y\lambda_0$.

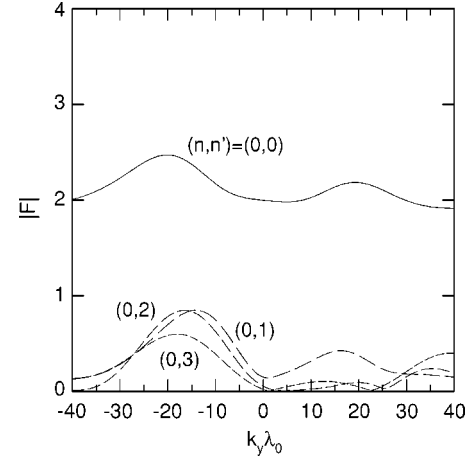


FIG. 3. For $\alpha=0$ and $\beta=0$, the form factor is plotted as a function of $k_y\lambda_0$.

These regions show where the plasmon, a coherent mode, has Landau damping corresponding to the transfer of energy to a SPE. In the SPE region, the imaginary part of the dielectric function is nonzero. However, not all intersubband single-particle transitions contribute to Landau damping as seen in Fig. 2. This is determined by the form factors in the response function. The $n=0 \rightarrow n'=2, 3$ single-particle transitions do not contribute to Landau damping. The collective plasmon branch in Fig. 2 is due to transitions from the ground subband below the Fermi energy to above and can be better understood by examining the response function $\chi^0(q_x, q_y; \omega)$ in the long wavelength limit. Setting $q_y=0$, it is a simple matter to show that

$$\chi^0(q_x, q_y=0; \omega)|_{\lambda_0/l_\alpha=0} = -\frac{1}{L_y} \sum_{k_y} \sum_{n' \geq 0} f_0(\epsilon_{k_y, n=0}) \times |F(q_x; k_y, n'; k_y, n=0)|^2 \frac{4n'}{\bar{\omega}^2 - 4n'^2}, \quad (9)$$

where $\epsilon_{k_y, n}$ are degenerate energy eigenvalues in the absence of SO coupling. Clearly the $n'=0$ term does not contribute to the response function and only intersubband transitions could give rise to a collective mode of finite frequency in the long wavelength limit. The intersubband transitions $n=0 \rightarrow n'=2$ and $n=0 \rightarrow n'=3$ also do not contribute to the collective plasma oscillation. This is the case for any E_F as long as only the ground subband is occupied. This is because the form factor $F(q_x; k_y - q_y, n'; k_y, n) = 0$ for $\alpha=0$ and $\beta=0$ for the transitions $n=0 \rightarrow n'=2, 3$. In the range of energies where the single-particle transitions have no Landau damping, we obtain a solution of the dispersion equation corresponding to an undamped collective plasma excitation. This result is stimulating in itself but we now discuss what effect the SO coupling has on these particle-hole modes and collective excitations.

In Fig. 3, we plot the form factor as a function of $k_y\lambda_0$ for $\lambda_0/l_\alpha=0.1$ and $\lambda_0/l_\beta=0.1$. The transitions are from the ground subband $n=0$ to $n'=0, 1, 2$, and 3. We chose $q_x\lambda_0$

$=0.1$ and $q_y\lambda_0=0.5$. Clearly, the intrasubband form factor is much larger than the intersubband form factor. Of course, the wave functions $\Phi_{\uparrow\downarrow}$ are normalized to unity which gives a value of $|F| \rightarrow 2$ for $|k_y\lambda_0| \gg 1$ when $n=n'$. We will use these results to determine how the SO coupling affects the Landau damping of the plasmons and what additional collective excitations are obtained as a result of the lifting of the spin degeneracy due to α coupling (see Fig. 1).

We have calculated the SPE energies when SO coupling is present and found features which are due to both α and β coupling. Setting $q_x=0$ in the polarization function, we obtain

$$\begin{aligned} \chi^0(q_x, q_y=0; \omega) = & -\frac{2}{L_y} \sum_{k_y} \sum_{n, n' \geq 0} \sum_{\sigma, \sigma'} f_0(\epsilon_{k_y, n, \sigma}) \\ & \times |F(q_x; k_y, n'; k_y, n)|^2 \\ & \times \frac{2(n' - n) + \sigma' \delta\epsilon_{k_y, n'} - \sigma \delta\epsilon_{k_y, n}}{\bar{\omega}^2 - [2(n' - n) + \sigma' \delta\epsilon_{k_y, n'} - \sigma \delta\epsilon_{k_y, n}]^2}. \end{aligned} \quad (10)$$

The only allowed transitions within an occupied subband are spin-flip transitions. For transitions between subbands, the spin orientation could remain unchanged. The energies of the single particle excitations for $q_y=0$ are given by the zeros of the denominator in Eq. (10), where k_y takes on a range of values with $|k_y| \leq k_{\sigma n}$ with $k_{\sigma n}$ determined from the following equation:

$$\frac{E_F}{\hbar\Omega/2} = k_{\sigma n}^2 \lambda_0^2 + 2n + 1 - \frac{1}{4} \left(\frac{k_{\sigma n} \lambda_0^2}{l_\beta} \right)^2 + \sigma \delta\epsilon_{k_{\sigma n}, n}. \quad (11)$$

When there is no SO coupling, there is only one particle-hole mode at $q_y=0$ for every allowed transition within a chosen subband or between a pair of subbands. However, with α coupling present there is a range of frequencies within each branch of the particle-hole mode region at $q_y=0$.

In Fig. 4, we plotted our results obtained by solving Eq. (7) at $T=0$ K. We chose $\lambda_0/l_\alpha=0.1$ and $\lambda_0/l_\beta=0.1$. Also, $\epsilon_b=13.0$ and $m^*=0.067m_e$, as appropriate for bulk GaAs, where m_e is the bare electron mass and $E_F/[\hbar\Omega/2]=2.0$. For this choice of E_F , only the ground subband is occupied at $T=0$ K. We also set $q_x\lambda_0=0.1$ and $\lambda_0=10.0a_B$, where a_B is the Bohr radius. We show both the particle-hole mode regions where Landau damping occurs and the undamped plasma excitations. Referring to the lowest two plasmon excitations, there is a plasmon branch lying just above the particle-hole mode region and another whose separation is much larger. This latter mode is the plasmon in Fig. 2 that is modified by the SO coupling. In the long wavelength limit, the depolarization shift for each mode initially decreases as q_y is increased. As a matter of fact, the energy of the second highest plasmon decreases as the wave vector q_y is increased and eventually anticrosses with the lowest plasmon mode. The negative dispersion for the second highest plasmon branch in the long wavelength limit is a new feature not present in Fig. 2 and is due to the dependence of the trans-

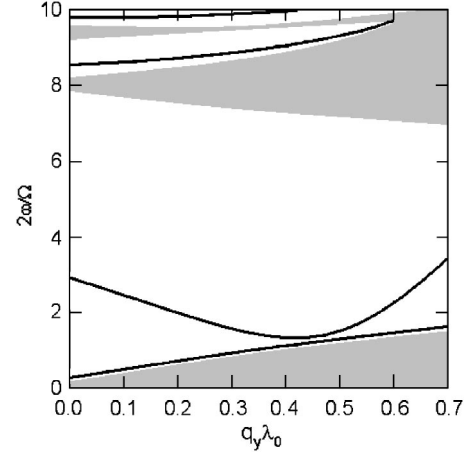


FIG. 4. The plasmon excitations and particle hole mode frequencies ω , in units of $\Omega/2$, are plotted as a function of $q_y\lambda_0$. The SPE's are shown as the shaded regions. The values for α , β , m^* , ϵ_b , and E_F are given in the text.

verse energy ϵ_x on the wave vector k_y arising from β coupling. Also, comparing Figs. 2 and 4, the SPE region with normalized frequency $\bar{\omega} \approx 2$ in the long wavelength limit $q_y\lambda_0 \ll 1$ does not give any Landau damping when there is SO coupling. Since only the lowest subband is occupied for our choice of E_F , the lowest plasmon mode corresponds to transitions within this subband ($n=n'=0$) and the higher modes correspond to transitions to higher subbands.

In addition to intrasubband excitations ($n=n'$ where the n th 1D subband is occupied), there are intersubband excitations ($n \neq n'$ where the n th 1D subband is occupied but the n' th 1D subband is unoccupied). These higher subband excitations are also shown in Fig. 4. There are two plasmon branches which split off from the particle-hole mode region near $\bar{\omega}=8$. These correspond to transitions from the ground subband to the $n'=4$ unoccupied subband, with and without the spins changing directions. There are also two distinct particle-hole mode regions near $\bar{\omega}=8$ corresponding to single-particle spin excitations $n=0 \rightarrow n'=4$. The particle-hole modes merge as q_y increases. The plasma modes lie above the particle-hole modes from which they are split as a result of the electrostatic interaction. At higher density, there are edge-state excitations ($n \neq n'$ where both n and n' 1D subbands are occupied).

IV. CONCLUDING REMARKS

In conclusion, our model for a quantum wire in conjunction with the RPA has successfully demonstrated some new features in the plasma excitation spectrum and SPE region due to SO coupling. Comparing Fig. 2 with Fig. 4, both the SPE's and plasmon modes are affected by the SO coupling. Our calculations yield plasmon branches which can be identified with intrasubband and intersubband transitions in the presence of SO coupling within a quantum wire. The plasmons may be observed in inelastic light scattering²⁰ and electron energy loss spectroscopy (EELS)²¹⁻²⁵ experiments, as was recently done for carbon nanotubes. A theoretical for-

mulation of EELS for quantum wires can be obtained in terms of the inverse dielectric function. The contribution to EELS from the SPE's and plasmons can be determined and the results compared with experiment. Our results were obtained for chosen material parameters and transverse wave vector q_x . However, our analysis of the excitation spectrum should not be affected for a different set of values.

ACKNOWLEDGMENTS

We acknowledge partial support from the National Science Foundation under Grant Nos. DMR-0303574 and CREST 0206162, PSC-CUNY Grant No. 65485-00-34 as well as Grant No. 4137308-04 from the NIH.

-
- ¹W. Hansen, M. Horst, J. P. Kotthaus, U. Merkt, Ch. Sikorski, and K. Ploog, *Phys. Rev. Lett.* **58**, 2586 (1987).
- ²T. Egeler, G. Abstreiter, G. Weimann, T. Demel, D. Heitmann, and P. Grambow, *Phys. Rev. Lett.* **65**, 1804 (1990).
- ³T. J. Thornton, M. Pepper, H. Ahmed, D. Andrews, and G. J. Davies, *Phys. Rev. Lett.* **56**, 1198 (1986).
- ⁴Q. Li and S. Das Sarma, *Phys. Rev. B* **41**, 10268 (1990).
- ⁵F. Hirler, J. Smoliner, E. Gornik, G. Weimann, and W. Schlapp, *Appl. Phys. Lett.* **57**, 261 (1990).
- ⁶R. R. Gerhardt, D. Weiss, and K. v. Klizing, *Phys. Rev. Lett.* **62**, 1173 (1989); R. W. Winkler, J. P. Kotthaus, and K. Ploog, *ibid.* **62**, 1177 (1989).
- ⁷C. W. J. Beenakker and H. van Houten, *Quantum Transport in Semiconductor Nanostructures*, Vol. 44 of *Solid State Physics* (Academic Press, New York, 1991).
- ⁸R. H. Yu and J. C. Hermanson, *Surf. Sci.* **276**, 369 (1992), and references therein.
- ⁹E. I. Rashba, *Fiz. Tverd. Tela (Leningrad)* **2**, 1224 (1960) [*Sov. Phys. Solid State* **2**, 1109 (1960)].
- ¹⁰Yu. A. Bychkov and E. I. Rashba, *Pis'ma Zh. Eksp. Teor. Fiz.* **39**, 66 (1984) [*JETP Lett.* **39**, 78 (1984)].
- ¹¹E. I. Rashba, *Usp. Fiz. Nauk* **84**, 557 (1964) [*Sov. Phys. Usp.* **7**, 823 (1965)].
- ¹²Yu. A. Bychkov and E. I. Rashba, *J. Phys. C* **17**, 6039 (1984).
- ¹³A. V. Moroz and C. H. W. Barnes, *Phys. Rev. B* **60**, 14 272 (1999).
- ¹⁴G. Gumbs and D. Huang, *J. Phys.: Condens. Matter* **4**, 1497 (1992).
- ¹⁵Danhong Huang and Shixun Zhou, *J. Phys.: Condens. Matter* **2**, 501 (1990).
- ¹⁶C. Ciuti, J. P. McGuire, and L. J. Sham, *Appl. Phys. Lett.* **81**, 4781 (2002); *Phys. Rev. Lett.* **89**, 156601 (2002).
- ¹⁷S. Datta and B. Das, *Appl. Phys. Lett.* **56**, 665 (1990); B. Das, S. Datta, and R. Reifenberger, *Phys. Rev. B* **41**, 8278 (1990).
- ¹⁸Junsaku Nitta, Tatsushi Akazaki, Hideaki Takayanagi, and Takatomo Enoki, *Phys. Rev. Lett.* **78**, 1335 (1997); *Phys. Rev. B* **55**, 9298 (1997).
- ¹⁹T. Hassenkam, S. Pedersen, K. Baklanov, A. Kristensen, C. B. Sorensen, P. E. Lindelof, F. G. Pikus, and G. E. Pikus, *Phys. Rev. B* **55**, 9298 (1997).
- ²⁰P. Chen, X. Wu, X. Sun, J. Lin, W. Ji, and K. L. Tan, *Phys. Rev. Lett.* **82**, 2548 (1999).
- ²¹R. Kuzuo, M. Tarauchi, and M. Tanaka, *Jpn. J. Appl. Phys., Part 2* **31**, L1484 (1992).
- ²²M. Kociak, L. Henrard, O. Stephan, K. Suenaga, and C. Colliex, *Phys. Rev. B* **61**, 13 936 (2000).
- ²³B. W. Reed and M. Sarikaya, *Phys. Rev. B* **64**, 195404 (2001), and references therein.
- ²⁴J. M. Pitarke, B. Pendry, and P. M. Echenique, *Phys. Rev. B* **55**, 9550 (1997).
- ²⁵J. G. F. Bertsch, H. Esbensen, and B. W. Reed, *Phys. Rev. B* **58**, 14 031 (1998).